Physics of Radioactive Beams[1]

Chapter 8

Pion Production

Carlos A. Bertulani, Texas A&M University-Commerce, TX 75429, USA

[1]These notes consist of a series of lectures presented by the author at the Geselschaft für Schwerionenforschung, Darmstadt, Germany in the Spring of 1994. GSI-Report 1994-11. This material was latter extended and published in the book "Physics of Radioactive Beams", C.A. Bertulani, M. Hussein and G. Muenzenberg, Nova Science, Hauppage, NY, 2002, ISBN: 1-59033-141-9

0.1 Introduction

We have seen that state-of-the-art self-consistent Hartree-Fock or shell model nuclear structure calculations are not able to correctly reproduce the binding energy of ^{11}Li or ^{14}Be. However, it is possible to numerically adjust the binding energy to the measured experimental values. In this case, one is able to reproduce the large observed interaction radii with reasonable accuracy [1]. The proton and neutron matter densities obtained in this way are represented by the solid lines in the lower part of Fig. 1(a).

Due to the small binding energy and the large spatial extension of the neutrons in the so-called "halo" [2], one expects the neutron momentum distribution to exhibit a smaller width than in more deeply bound nuclei. This has indeed been observed in several ways.

Kobayashi et al. [3] observed the fragmentation of ^{11}Li with a radioactive beam of energy 790 MeV/nucleon. Their experimental data for the transverse momentum distribution of ^{9}Li from the reaction $^{11}\text{Li} \rightarrow {}^{9}\text{Li} + 2\text{n}$ can be found in the bottom half of Fig. 1(b). It can be fitted with a superposition of two Gaussian distributions of widths $\omega_{\text{core}} = 95 \pm 12$ MeV/c and $\omega_{\text{halo}} = 23 \pm 5$ MeV/c. By using Goldhaber's statistical model of the fragmentation process [4], they were able to interpret the two widths as an indication that the neutron momentum distribution inside the halo and the core of ^{11}Li are different. However, alternative explanations of the two-widths shape of the transverse momentum distribution are possible [5],. It is therefore wise to pursue other complementary ways of determining the momentum and coordinate space structure of exotic nuclei. For example, one can also measure the neutron momentum distribution in ^{11}Li by detecting the neutrons from the decay of ^{11}Li [6, 7].

We will investigate the possibility to further determine the coordinate and momentum space distribution of neutrons inside weakly bound isotope via pion production with radioactive beams. In principle, pion production in nucleus-nucleus collisions can be described with nuclear transport models developed during the last decade [8, 9, 10]. These models have been very successful to describe particle production in heavy ion collisions. The most used model is based on the BUU equation. However, they are semi-classical in nature and therefore lack the capability to properly take into account the special nuclear structure features of weakly bound nuclei near the drip line. It is therefore necessary to construct a more phenomenological model. The model is not able to provide a complete time dependent description of heavy ion reactions the way the above mentioned transport models can. But it is more precise as far as utilizing nuclear structure information is concerned. Before, we have shown a calculation similar to the ones presented in Refs. [12, 13, 14], but using shell model nucleon densities and energy dependent cross sections. The calculations are to due to Li, Bauer and Hussein [14].

Supplement A

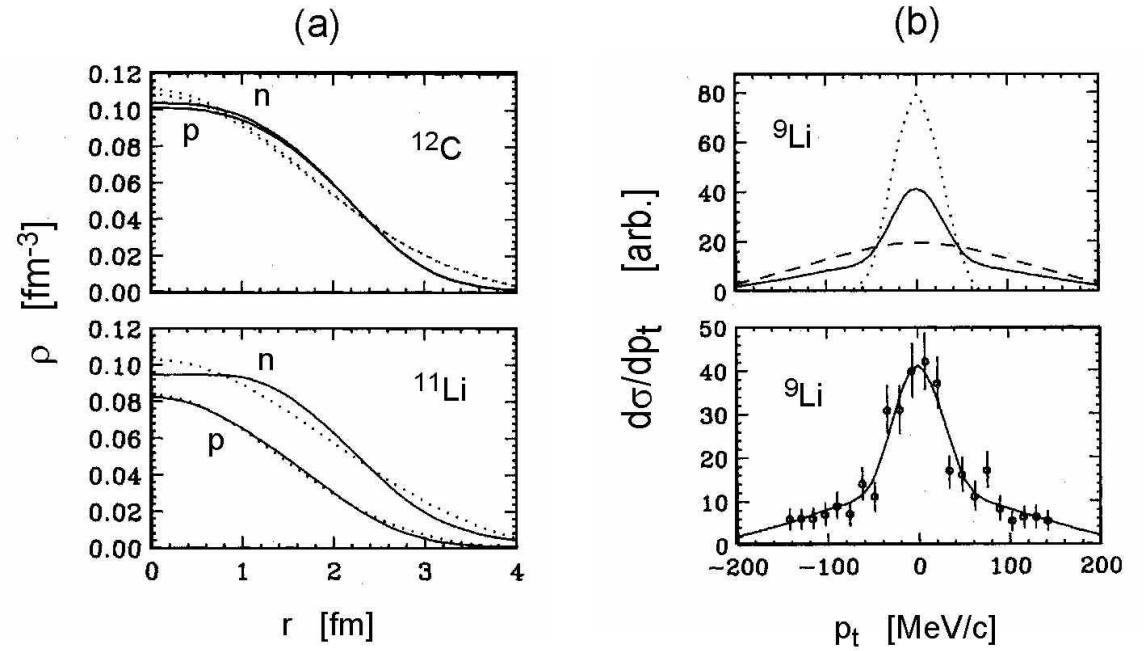

Figure 1: (a) Density distributions for ^{12}C and ^{11}Li. The solid lines are calculated with the binding energy adjusted shell model. The dotted lines are the Gaussian fits to the density profiles. (b) Upper figure: Calculated transverse momentum distribution of ^{9}Li in the reaction ^{11}Li+^{12}C $\rightarrow$ ^{9}Li+2n+X. The dashed (dotted) line is obtained by assuming knock out of two neutrons from the core (halo) of ^{11}Li. The solid line represents the weighted sum of the two. Lower figure: Comparison with the experimental data.

0.2 The Boltzmann equation for nucleon-nucleon collisions

Let us call $dN\left(\mathbf{r},\mathbf{p},t\right)$ the number of particles with positions $\mathbf{r}$ and momenta $\mathbf{p}$ at time t. If dN is the number of particles in the volume element d^3r and whose momenta fall in the momentum element d^3p at time t, then the *distribution function* $f\left(\mathbf{r},\mathbf{p},t\right)$ is given by

$$dN = f\left(\mathbf{r},\mathbf{p},t\right) d^3r d^3p \tag{1}$$

For a particle to be included in dN its position coordinates must lie between $\mathbf{r}_i$ and $\mathbf{r}_i + \Delta\mathbf{r}_i$, and its momentum must lie between $\mathbf{p}_i$ and $\mathbf{p}_i + \Delta\mathbf{p}_i$, where i runs from 1 to 3.

If there were no collisions, then a short time Δt later each particle would move from to $\mathbf{r} + \Delta\mathbf{r}$, and each particle momentum would change from to $\mathbf{p} + \mathbf{F}\Delta t$, where is $\mathbf{F}$ the external force on a particle at r with momentum $\mathbf{p}$. Therefore, any difference between $dN\left(\mathbf{r},\mathbf{p},t\right)$ and

$dN\left(\mathbf{r}+\mathbf{\Delta r},\mathbf{p}+\mathbf{F}\Delta t,t\right)$ is due to collisions, and we may set

$$\left[f\left(\mathbf{r}+\mathbf{\Delta r},\mathbf{p}+\mathbf{F}\Delta t,t\right)-f\left(\mathbf{r},\mathbf{p},t\right)\right]d^3rd^3p=\left(\frac{\partial f}{\partial t}\right)_c d^3r'd^3p'\Delta t\ , \tag{2}$$

where $\left(\partial f/\partial t\right)_c$ is the time rate of change of f due to collisions. Expanding the first term on the left as a Taylor series about $f\left(\mathbf{r},\mathbf{p},t\right)$, we have (here repeated indices mean a summation, e.g., $a_ib_i=\mathbf{a}\cdot\mathbf{b}=a_1b_1+a_2b_2+a_3b_3$)

$$f\left(\mathbf{r}+\mathbf{\Delta r},\mathbf{p}+\mathbf{F}\Delta t,t\right)=f\left(\mathbf{r},\mathbf{p},t\right)+\left(\frac{\partial f}{\partial r_i}\frac{p_i}{m}+\frac{\partial f}{\partial p_i}F_i+\frac{\partial f}{\partial t}\right)\Delta t\ , \tag{3}$$

where m is the nucleon mass.

In the limit as $\Delta t\rightarrow 0$,

$$\frac{\partial f}{\partial r_i}\frac{p_i}{m}+\frac{\partial f}{\partial p_i}F_i+\frac{\partial f}{\partial t}=\left(\frac{\partial f}{\partial t}\right)_c \tag{4}$$

which is known at the *Boltzmann equation* for f. Note we have used the result that the Jacobian for the transformation $d^3r'd^3p'=\left|J\right|d^3rd^3p$ is unity, where J is the 6×6 element array,

$$J=\frac{\partial\left(x,y,z,p_x,p_y,p_z\right)}{\partial\left(x',y',z',p'_x,p'_y,p'_z\right)}\ . \tag{5}$$

This assumption is valid only if the collisions are elastic, i.e., if they conserve energy and momentum.

The system of nucleons are often free from external sources, so that one can drop off the term containing F_i in Eq. 4. However, to account for the effect of each particle interacting with all other, one introduces the concept of mean-field, $U\left(\mathbf{r},\mathbf{p},t\right)$. This mean-field exerts a force on each particle, given by $-\nabla_{\mathbf{r}}U\left(\mathbf{r},\mathbf{p},t\right)$. Re-deriving Eq. 4 in terms of a mean field yields

$$\frac{\partial f}{\partial t}+\left(\frac{\mathbf{p}}{m}+\nabla_{\mathbf{p}}U\right)\cdot\nabla_{\mathbf{r}}f-\nabla_{\mathbf{r}}U\cdot\nabla_{\mathbf{r}}f=\left(\frac{\partial f}{\partial t}\right)_c \tag{6}$$

Note that the left hand side of this equation is simply the total time derivative of the distribution function, Df/Dt. In the absence of collisions, one obtains the *Vlasov equation*

$$\frac{Df}{Dt}=\frac{\partial f}{\partial t}+\left(\frac{\mathbf{p}}{m}+\nabla_{\mathbf{p}}U\right)\cdot\nabla_{\mathbf{r}}f-\nabla_{\mathbf{r}}U\cdot\nabla_{\mathbf{r}}f=0. \tag{7}$$

Let us now assume that the system of nucleons form a dilute system of particles. Dilute means that the total volume of the gas particles is small compared to the volume available to the gas,

$$na^2\ll 1 \tag{8}$$

where n is the number density of particles and a is the radius of a particle. Since the particles in a neutral gas do not have long range forces like the particles in a plasma, they are assumed to

interact only when they collide, i.e., when the separation between two particles is not much larger than $2a$. The term collision normally means the interaction between two such nearby particles. A particle moves in a straight line between collisions. The average distance traveled by a particle between two collisions is known as the mean free path. The mean free path depends on the cross section σ, and is given by

$$\lambda = \frac{1}{n\sigma}. \tag{9}$$

One consequence of the requirement that the gas be dilute is that $\lambda \gg a$. In other words the diluteness implies that the mean free path is much larger than the particle size so that a typical particle trajectory consists of long straight segments interrupted by almost discontinuous changes of direction when collisions occur. If the gas is dilute, the probability of three body collisions is much lower than for two body collisions and they can be neglected.

The Vlasov equation, $Df/Dt = 0$, says that f does not change as we move along the trajectory of a particle, provided collisions are neglected. Collisions can change f in two ways.

1. Some particles originally having momentum $\mathbf{p}$ will have some different momentum after the collision. This causes a decrease in f.

2. Some particles having other momentum may have the momentum $\mathbf{p}$ after a collision, increasing f.

The Boltzmann collisional term in the Boltzmann equation can be written as

$$\frac{Df}{Dt} d^3r d^3p = C_{in} - C_{out} \tag{10}$$

where C_{in} and C_{out} are the rates at which particles enter and leave the infinitesimal volume $d^3r d^3p$ due to collisions.

Suppose two particle with initial velocities $\mathbf{v}_1$and $\mathbf{v}_2$ have velocities $\mathbf{v}_1'$and $\mathbf{v}_2'$ and after a collision. Since all particles have the same mass, conservation of momentum and energy require that

$$\mathbf{v}_1' + \mathbf{v}_2' = \mathbf{v}_1 + \mathbf{v}_2 \quad \text{and} \quad \frac{1}{2}\left|\mathbf{v}_1'\right|^2 + \frac{1}{2}\left|\mathbf{v}_2'\right|^2 = \frac{1}{2}\left|\mathbf{v}_1\right|^2 + \frac{1}{2}\left|\mathbf{v}_2\right|^2 \tag{11}$$

One would like to calculate the final velocities $\mathbf{v}_1'$and $\mathbf{v}_2'$ from the initial velocities. Since and have six components we need six equations to solve for them. Four are provided by the conservation equations. A fifth condition comes from the fact that collisions are coplanar if the forces between particles are purely radial, i.e., $\mathbf{v}_1'$ will lie in the plane of $\mathbf{v}_1$and $\mathbf{v}_2$, forcing $\mathbf{v}_2'$ to also lie in the same plane from conservation of momentum. We still need a sixth condition, which must come from the nature of the force between the particles. The short range nature of the forces allow us to assume that the collision occurs at essentially only one value of $\mathbf{r}$ so we need not account for the changes of external forces. The unknown velocities are therefore specified once the impact

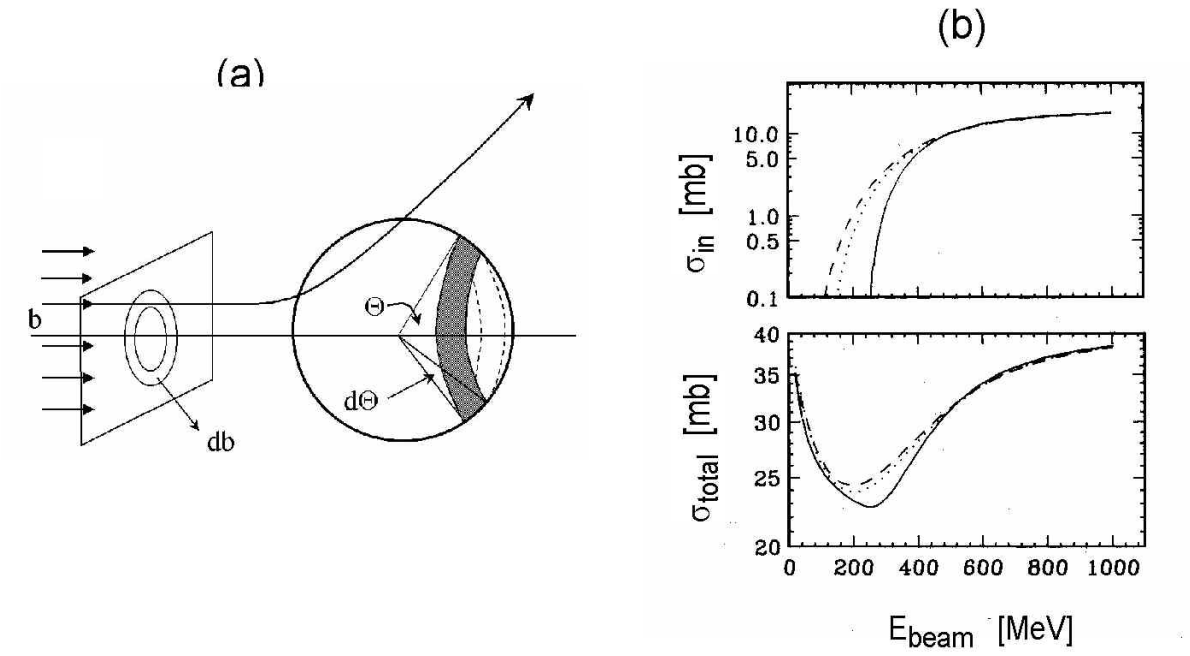

Figure 2: (a) Scattering of an incident beam of particles by a center of force. The impact parameter is b, and the angle of deflection is Θ. The number of particles scattered into a solid angle $d\Omega = 2\pi \sin\Theta d\Theta$ lying between Θ and $\Theta + d\Theta$ must equal the number scattered through impact parameters between $b$and $b + db$, hence $2\pi bdb = 2\pi\sigma(\Theta)\sin\Theta d\Theta$. (b) Nucleon momentum averaged nucleon-nucleon cross sections in the reaction ^{11} Li+^{12}C. Solid lines are the free space nucleon-nucleon cross sections. Dotted lines are for carbon nucleons colliding with halo neutrons and dashed lines are for carbon nucleons colliding with core nucleons of ^{11} Li.

parameter $\mathbf{b}$ and the azimuthal orientation ϕ of the collision is known. For an elastic collision the magnitude of the relative velocity is a collisional invariant:

$$|\mathbf{v}_1' - \mathbf{v}_2'| = |\mathbf{v}_1 - \mathbf{v}_2|\,, \tag{12}$$

which follows from kinetic energy conservation in the center of mass frame. Thus we may specify the remaining two pieces of information concerning the collision in terms of the change of the orientation of the relative velocity, i.e., in terms of two angles Θ and ϕ. In an elastic encounter the collision occurs in a single plane $\phi = const.$, turning the relative velocity $\mathbf{v}_1 - \mathbf{v}_2$ through an angle Θ without change in the magnitude of the relative velocity. For given intermolecular forces, the deflection, Θ, depends only on the impact parameter b. The differential cross-section for the encounter $\sigma(\mathbf{v}_1, \mathbf{v}_2|\mathbf{v}_1', \mathbf{v}_2')$ is defined so that $\sigma d\Omega = bdbd\phi$, where $d\Omega = 2\pi\sin\Theta d\Theta$.

Consider a beam of particles of number density n_1 and velocity $\mathbf{v}_1$ colliding with another beam of particles of density n_2 and velocity $\mathbf{v}_2$. A particle in the second beam experiences a flux

$I = n_1 |\mathbf{v}_1 - \mathbf{v}_2|$ of particles from the first beam. We consider the number δn_c of collisions per unit time per unit volume which deflect particles from the second beam into a solid angle $d\Omega$,

$$\delta n_c = \sigma (\mathbf{v}_1, \mathbf{v}_2 | \mathbf{v}_1', \mathbf{v}_2') \, n_1 |\mathbf{v}_1 - \mathbf{v}_2| \, n_2 d\Omega. \tag{13}$$

Consider the inverse collision where $(\mathbf{v}_1, \mathbf{v}_2) \longrightarrow (\mathbf{v}_1', \mathbf{v}_2')$. If the molecular processes are time-reversible, then we expect the reverse cross-section to equal the forward cross-section:

$$\sigma (\mathbf{v}_1', \mathbf{v}_2' | \mathbf{v}_1, \mathbf{v}_2) = \sigma (\mathbf{v}_1, \mathbf{v}_2 | \mathbf{v}_1', \mathbf{v}_2') \tag{14}$$

It should be noted that this condition of time reversibility is by no means self-evident.

We now evaluate the term C_{out}. Consider the two streams of particles having the tips of their momentum vectors in d^3p_1 and d^3p_2. The first stream makes up a beam of number density $n_1 = f(\mathbf{r}, \mathbf{p}_1, t) \, d^3p_1$, and velocity $\mathbf{v}_1$, whereas the second stream constitutes a beam of density $n_2 = f(\mathbf{r}, \mathbf{p}_2, t) \, d^3p_2$ and velocity $\mathbf{v}_2$. Substitution for n_1 and n_2 in the collision rate between the two beams is

$$\delta n_c = \sigma (\mathbf{v}_1, \mathbf{v}_2 | \mathbf{v}_1', \mathbf{v}_2') \, |\mathbf{v}_1 - \mathbf{v}_2| \, f(\mathbf{r}, \mathbf{p}_1, t) \, f(\mathbf{r}, \mathbf{p}_2, t) \, d\Omega d^3p_1 d^3p_2. \tag{15}$$

Since C_{out} must be equal to the number of collisions per unit time with the volume $d^3r_1 d^3p_1$, C_{out} is obtained by multiplying δn_c by d^3r_1 and then integrating over all solid angles, Ω, and collision partner momenta, p_2. Hence,

$$\begin{aligned} C_{out} &= d^3r_1 \int_{p_2} \int_{\Omega} \delta n_c \\ &= d^3r_1 d^3p_1 \int d^3p_2 \int d\Omega \sigma (\mathbf{v}_1, \mathbf{v}_2 | \mathbf{v}_1', \mathbf{v}_2') \, |\mathbf{v}_1 - \mathbf{v}_2| \, f(\mathbf{r}, \mathbf{p}_1, t) \, f(\mathbf{r}, \mathbf{p}_2, t) \, . \end{aligned} \tag{16}$$

To evaluate C_{in}, we consider the reverse collisions between particles in d^3p_1' and with momenta in d^3p_2' such that their velocities after collisions lie within $d^3p_1$and d^3p_2, respectively. The number of such collision per unit volume per unit time is

$$\delta n_c' = \sigma (\mathbf{v}_1', \mathbf{v}_2' | \mathbf{v}_1, \mathbf{v}_2) \, |\mathbf{v}_1' - \mathbf{v}_2'| \, f(\mathbf{r}, \mathbf{p}_1', t) \, f(\mathbf{r}, \mathbf{p}_2', t) \, d\Omega d^3p_1' d^3p_2'. \tag{17}$$

Recall that the relative velocity of the particles is a collisional invariant, $|\mathbf{v}_1' - \mathbf{v}_2'| = |\mathbf{v}_1 - \mathbf{v}_2|$, and from *Liouville's theorem*, if the interaction can be described by a Hamiltonian,

$$d^3p_1' d^3p_2' = d^3p_1 d^3p_2 \tag{18}$$

Thus assuming reversible collisions, the invariance of the relative velocity and the constant phase space volume,

$$\delta n_c' = \sigma (\mathbf{v}_1, \mathbf{v}_2 | \mathbf{v}_1', \mathbf{v}_2') \, |\mathbf{v}_1 - \mathbf{v}_2| \, f(\mathbf{r}, \mathbf{p}_1', t) \, f(\mathbf{r}, \mathbf{p}_2', t) \, d\Omega d^3p_1 d^3p_2. \tag{19}$$

The term is C_{in} obtained by multiplying $\delta n_c'$ by $d^3r_1$and integrating over all solid angles, Ω, and collision partner momenta, $\mathbf{p}_2$., i.e.,

$$C_{out} = d^3r_1 d^3p_1 \int d^3p_2 \int d\Omega\sigma\left(\mathbf{v}_1, \mathbf{v}_2|\mathbf{v}_1', \mathbf{v}_2'\right)|\mathbf{v}_1 - \mathbf{v}_2| f\left(\mathbf{r}, \mathbf{p}_1', t\right) f\left(\mathbf{r}, \mathbf{p}_2', t\right). \tag{20}$$

Now that we have the rates at which particles leave and enter $d^3r_1d^3p_1$ we can write the full *Boltzmann equation* as

$$\begin{aligned}
&\frac{\partial f}{\partial t} + \left(\frac{\mathbf{p}}{m} + \nabla_{\mathbf{p}} U\right) \cdot \nabla_{\mathbf{r}} f - \nabla_{\mathbf{r}} U \cdot \nabla_{\mathbf{r}} f = \\
&\int d^3p_2 \int d\Omega\sigma\left(\mathbf{v}_1, \mathbf{v}_2|\mathbf{v}_1', \mathbf{v}_2'\right)|\mathbf{v}_1 - \mathbf{v}_2| \\
&\times \left[f\left(\mathbf{r}, \mathbf{p}_1', t\right) f\left(\mathbf{r}, \mathbf{p}_2', t\right) - f\left(\mathbf{r}, \mathbf{p}_1, t\right) f\left(\mathbf{r}, \mathbf{p}_2, t\right)\right].
\end{aligned} \tag{21}$$

which is conveniently abbreviated as

$$\frac{\partial f}{\partial t} + \left(\frac{\mathbf{p}}{m} + \nabla_{\mathbf{p}} U\right) \cdot \nabla_{\mathbf{r}} f - \nabla_{\mathbf{r}} U \cdot \nabla_{\mathbf{r}} f = \int d^3p_2 \int d\Omega\sigma\left(\Omega\right)|\mathbf{v}_1 - \mathbf{v}_2|\left[f_1' f_2' - f_1 f_2\right]. \tag{22}$$

We have assumed that the differential cross-section is a function only of the scattering angle Ω between $\mathbf{p}_1$ and $\mathbf{p}_2$, since the differential cross-section for a simple spherically symmetric interaction potential can, due to symmetry, only be a function of the scattering angle. The complete (classical) Boltzmann equation with the collision integral for binary collisions is a nonlinear integro-differential equation for the distribution function.

For a system of nucleons the classical Boltzmann equation can be modified to account for the Pauli principle. The principle states that no nucleon can scatter into a phase space already occupied by another nucleon. This amounts in modifying the term $f_1 f_2$ to $f_1 f_2 \left[1 - f_1'\right]\left[1 - f_2'\right]$, where the $1 - f'$ terms is zero if the final state is occupied ($f = 1$). Accordingly, $f_1' f_2'$ is modified to $f_1' f_2' \left[1 - f_1\right]\left[1 - f_2\right]$. Thus, for a nucleon system of particles, the appropriate Boltzmann equation for a nucleon-nucleon collisions (called the *Boltzmann-Uehling-Uhlenbeck*, or *BUU*, equation) is

$$\begin{aligned}
&\frac{\partial f}{\partial t} + \left(\frac{\mathbf{p}}{m} + \nabla_{\mathbf{p}} U\right) \cdot \nabla_{\mathbf{r}} f - \nabla_{\mathbf{r}} U \cdot \nabla_{\mathbf{r}} f = \\
&\int d^3p_2 \int d\Omega\sigma_{NN}\left(\Omega\right)|\mathbf{v}_1 - \mathbf{v}_2| \\
&\times \left\{f_1' f_2'\left[1 - f_1\right]\left[1 - f_2\right] - f_1 f_2\left[1 - f_1'\right]\left[1 - f_2'\right]\right\}.
\end{aligned} \tag{23}$$

The collision integral, Eq.23, takes into account the nucleon scattering inside the nuclear medium. Its form can be justified on general physical grounds, but it can be also derived self-consistently from the quantum equations of motion of the one-body and two-body density .

Eq. 23 needs as basic ingredients the mean field U and the cross section σ_{NN}. Because these two quantities are related to each other, one should in principle derive them in a self-consistent

microscopic approach, as the Brueckner theory. However, in practice the simulations are often done with a phenomenological mean field and free nuclear cross sections.

The most commonly used mean field is of Skyrme-type, eventually with a momentum dependent part [15].

The output of Eq. 23 is the distribution function $f(r,p,t)$, which allows one to calculate a lot of properties of the heavy-ion collisions. Let us quote collective flows, proton and neutron production rates, (sub-threshold and above threshold) pion and kaon yields, etc. Combining Eq. 23 with a phase-space coalescence model, one can also calculate such quantities as exclusive flows and intermediate fragment formations.

In order to numerically solve Eq. 23 one needs to go throughout the following general steps: initialization, mean field propagation, collisions and Pauli blocking. The solution of 23 is usually Monte Carlo simulated by using the pseudo-particle method. According to these models the dynamics is traced by the one-body distribution function $f(\mathbf{r},\mathbf{p},t)$ expanded in terms of a set of generating functions centered on a finite number of points, Monte Carlo distributed in the whole phase-space. In this way the dynamics of nucleons is replaced by the dynamics of test-particles. Between two collisions a test-particle propagates following a classical trajectory determined by Newton-type equations. In order to have a good approximation of the exact continuous distribution function,$f(\mathbf{r},\mathbf{p},t)$, the number of test-particles per nucleon should be large enough. This requirement brings about, in the case of a large nucleus, a fast increase of the CPU time needed for running serial-code simulations.

Let us briefly discuss the general aspects of a typical numerical algorithm. In the first step one prepares nuclei in the ground state by discretizing the continuous distribution function as a sum of elementary functions. Here we describe them in terms of Gaussian functions both in coordinate and momentum space, with fixed widths σ_r and σ_p:

$$f(\mathbf{r},\mathbf{p},t)=\frac{1}{n_g\left(4\pi^2\sigma_r\sigma_p\right)^{3/2}}\sum_{i=1,n}\exp\left[-\left(\mathbf{r}-\mathbf{r}_i\right)^2/2\sigma_r^2\right]\exp\left[-\left(\mathbf{p}-\mathbf{p}_i\right)^2/2\sigma_p^2\right] \qquad (24)$$

where n_g is the number of generating functions per nucleon. This number should be quite large in order to have a good approximation of the exact continuous distribution function $f(\mathbf{r},\mathbf{p},t)$. The total number of test-particles ("Gaussians") is $N=n_gA$, where A is the total number of nucleons in the nuclear system. The ground state is prepared by a Monte Carlo sampling of the phase space with a variational self- consistent procedure to reproduce the nuclear binding energy.

Once the initial phase-space configuration of the test particles in the two ground state nuclei is fixed, the two nuclei are translated and boosted to the center of mass frame where the calculation is performed. The evolution in time of the system is controlled by dividing the total reaction time in small time steps, dt (of the order of 0.5 fm/c). During a time step interval the test-particles are propagated freely in phase-space along the classical trajectories determined by the Newton equations, with the force term given by the derivative of the mean field. Actually, in the case of Gaussian generating functions (Eq. 24), it can be shown [16] that the dynamics of test-particles ("the Gaussians") is given by Ehrenfest type equations, with the force term replaced by

the convoluted derivatives of the mean field over the given Gaussian:

$$\frac{d\mathbf{r}_i}{dt} = \frac{\mathbf{p}_i}{m} + \langle \nabla_p U(\mathbf{r},\mathbf{p}) \rangle_{\mathbf{r}_i,\mathbf{p}_i} \qquad \text{and} \quad \frac{d\mathbf{p}_i}{dt} = \frac{\mathbf{r}_i}{m} + \langle \nabla_r U(\mathbf{r},\mathbf{p}) \rangle_{\mathbf{r}_i,\mathbf{p}_i} . \tag{25}$$

At the end of each time-step the phase space is searched for allowed collisions. The algorithm for simulating the collision integral is based on the mean free path, λ. The procedure is as follow [11]: for a given test particle one searches a possible scattering partner taken as the closest test-particle inside a sphere of a given radius. Then one estimates the averaged mean free path as $\lambda = (\rho\sigma)^{-1}$, where ρ is the local averaged density and is σ the cross section corresponding to the relative kinetic energy of the partners. Dividing the calculated mean free path by the relative velocity of the two test particles, one finds the averaged time-life between two collisions, dt_{coll}. In terms of dt_{coll} the probability for scattering is :

$$P = 1 - \exp\left(-dt/dt_{coll}\right) . \tag{26}$$

If dt is chosen as to have $dt << dt_{coll}$ then P can be approximated by dt/dt_{coll}. After the probability P is calculated the decision for the scattering is made by the Monte Carlo method: the scattering is decided if P is greater than a generated random number smaller than one. As soon as a collision is decided, the final momenta of the two scattered test-particles are randomly generated, with the momentum-energy conservation constraints. The final decision for the scattering is taken only if the final scattering states are not Pauli-blocked. The Pauli-blocking factor is , $(1-f_1)(1-f_2)$ where f_1 and f_2 are the one-body distribution functions calculated in the phase-space points corresponding to the final states of the scattered test-particles. The decision about the Pauli-blocking is taken again by Monte Carlo method.

0.3 Inclusive π^+ and π^- production cross section

Within a Glauber-type multiple collision model, the total number of nucleon-nucleon collisions in the reaction of $A + B$ at an impact parameter b is

$$N(b) = \overline{\sigma}(E) \int_{\mathcal{O}} dxdy \int dz_1 dz_2 \rho_A(x,y,z_1)\rho_B(x,y-b,z_2), \tag{27}$$

where $\mathcal{O}$ is the overlap region of nuclei A and B, and $\overline{\sigma}(E)$ is the momentum averaged total nucleon-nucleon cross section. Since the core nucleons and the halo neutrons have different momentum distributions in ^{11}Li, $\overline{\sigma}(E)$ may be written as

$$\overline{\sigma}(E) = \tfrac{9}{11}\overline{\sigma}_{\rm core}(E) + \tfrac{2}{11}\overline{\sigma}_{\rm halo}(E). \tag{28}$$

Since we wish to analytically carry out the bulk of the calculations, we follow Karol [17] and assume that the nucleon density distribution is a Gaussian function

$$\rho(r) = \rho(0)\, \exp\left(-\frac{r^2}{a^2}\right). \tag{29}$$

The integration in Eq. 27 can then be performed analytically to yield the result

$$N(b) = \frac{\overline{\sigma}(E)\pi^2\rho_A(0)\rho_B(0)a_A^3a_B^3}{a_A^2+a_B^2}\exp\left(-\frac{b^2}{a_A^2+A_B^2}\right). \tag{30}$$

Similar forms for the proton-proton and neutron-neutron collision numbers can be obtained in terms of their density distribution parameters.

Under the assumption that pions are produced through Δ resonances, the inclusive π^+ and π^- cross sections can then be written as [13]

$$\begin{aligned}\frac{d\sigma_{\rm inc}^{\pi^+}}{d\Omega} &= |f_{N\Delta}(q)|^2 Z_A Z_B \frac{\pi^2\rho_{ZA}(0)\rho_{ZB}(0)a_{ZA}^3a_{ZB}^3}{a_{ZA}^2+a_{ZB}^2} \\ &\times 2\pi\int_0^\infty bdb\exp\left[-\frac{b^2}{a_{ZA}^2+a_{ZB}^2}-\frac{\overline{\sigma}(E)(AB-1)\rho_A(0)\rho_B(0)a_A^3a_B^3}{a_A^2+a_B^2}\right. \\ &\left.\exp\left(-\frac{b^2}{a_A^2+a_B^2}\right)\right], \end{aligned} \tag{31}$$

$$\begin{aligned}\frac{d\sigma_{\rm inc}^{\pi^-}}{d\Omega} &= |f_{N\Delta}(q)|^2 N_A N_B \frac{\pi^2\rho_{NA}(0)\rho_{NB}(0)a_{NA}^3a_{NB}^3}{a_{NA}^2+a_{NB}^2} \\ &\times 2\pi\int_0^\infty bdb\exp\left[-\frac{b^2}{a_{NA}^2+a_{NB}^2}-\frac{\overline{\sigma}(E)(AB-1)\rho_A(0)\rho_B(0)a_A^3a_B^3}{a_A^2+a_B^2}\right. \\ &\left.\exp\left(-\frac{b^2}{a_A^2+a_B^2}\right)\right], \end{aligned} \tag{32}$$

where ρ_{Ni} and ρ_{Zi} are the neutron and proton coordinate space densities of nucleus i, and $f_{N\Delta}(q)$ is the amplitude for the process $N+N \rightarrow N+\Delta$. The exponentials inside the integrals represent the product of the proton (Eq. 31) or neutron (Eq. 32) densities with the elastic survival probability given by $\exp[-\left(\overline{\sigma}(E)(AB-1)\rho_A(0)\rho_B(0)a_A^3a_B^3\right)/\left(a_A^2+a_B^2\right)\exp\left(-b^2/\left(a_A^2+a_B^2\right)\right)]$,.

At beam energies smaller than 1 GeV/nucleon, available experimental data [18, 19] show that pion are mainly produced through Δ resonances. Direct processes of the form $N+N \rightarrow N+N+\pi$ account for less than 20 percent and higher resonances have negligible cross sections.

From the experimental data of n+p collisions [18] and the calculated ratio of the isospin matrix elements [13], it can be shown that the numbers of π^+ and π^- produced in n+p collisions are smaller than that in p+p and n+n collisions, respectively, by about an order of magnitude. We therefore expect that the above equations are good approximations for the present purpose of this calculation.

The above considerations do not include the effect of the Pauli-exclusion principle on the final state nucleons after producing the pions. This should result in a reduction of $|f_{N\Delta}(q)|^2$ in the nuclear medium. However, to first approximation, this reduction should be the same

for both pion species, and since we are only interested in the ratio of the production cross sections, the reduction factor will cancel out.

Pion reabsorption accounts for up to 50% of the produced primordial pions in the light systems studied here [9]. In the same spirit as just described for the Pauli exclusion principle, the amplitudes $f_{N\Delta}$ should be understood as effective amplitudes which already include this reduction.

Since we are interested in the ratio of the inclusive π^+ and π^- production, the main ingredients in the model calculation are then the density parameters and the momentum averaged cross sections.

We start out by looking for realistic density distributions for protons and neutrons for all isotopes under consideration. This is accomplished by using a binding energy adjusted shell model program [1]. As examples for the calculated density distributions, we display in Fig. 1(a) the neutron and proton densities for ^{12}C (upper part) and ^{11}Li (lower part) by the solid lines.

The results of the Gaussian fit to the calculated density distributions are represented by the dotted lines. In Table 9.1, we list the obtained values for $\rho(0)$ and a for proton and neutron density distributions for all Li-isotopes used in the subsequent calculations as well as the corresponding values for ^{12}C.

	$\rho_n(0)$ (fm^{-3})	a_n (fm)	$\rho_p(0)$ (fm^{-3})	a_p (fm)	$\rho(0)$ (fm^{-3})	a (fm)
^{12}C	0.1148	2.110	0.1120	2.128	0.2268	2.120
^{7}Li	0.1051	1.897	0.1121	1.688	0.2168	1.797
^{8}Li	0.1151	1.984	0.0996	1.755	0.2134	1.885
^{9}Li	0.1215	2.071	0.0989	1.760	0.2178	1.952
^{11}Li	0.1115	2.346	0.0851	1.851	0.1922	2.175

Table 9.1: Parameters of the Gaussian fits to the nucleon density distributions in Li-isotopes and ^{12}C.

For calculating the momentum averaged nucleon-nucleon cross sections, one chooses the momentum space distribution functions such that the results agree with know experimental data.

One such comparison is performed in Fig. 1(b). In the upper part, one uses a Fermi gas model for the momentum distribution of the neutrons in ^{11}Li. One assumes different Fermi momenta for core and halo neutrons. The fitted values are P_F(core) = 158 MeV/c and P_F(halo) = 38 MeV/c which coincide with the one inferred from the experimental data by using the Goldhaber model. By randomly picking 2 neutron momenta from within these Fermi spheres and adding their momenta, one obtains a recoil spectrum for ^{9}Li in the projectile rest frame, employing the assumptions entering the Goldhaber model [4]. By picking two neutrons from the halo, one obtains the dotted curve in Fig. 1(b). The dashed

curve is the result of using the same procedure on two core neutrons. The solid curve is the result of an addition of the two contributions with the proper weights as measured in the experiment of Kobayashi et al. [3]. For purposes of comparison, all curves in the upper part of Fig. 1(b) were normalized to the same value. In the lower part of this figure, we compare the simulated ^{9}Li transverse momentum spectra to the data of Kobayashi et al. [3]. One can see that one is able to reliably fit the experimental observables.

We obtain the momentum distribution averaged nucleon-nucleon cross sections by integrating $\sigma(\sqrt{s})$ weighted with the momentum distributions of target and projectile,

$$\overline{\sigma}(E_{\rm beam}) = \int f_A(\mathbf{p}_A) f_B(\mathbf{p}_B - \mathbf{p}_{\rm beam}) \sigma(\sqrt{s}(\mathbf{p}_A, \mathbf{p}_B)) d^3p_A d^3p_B. \tag{33}$$

Here, $f_i(\mathbf{p})$ are the momentum distributions of target ($i = A$) and projectile $i = B$.

For the purpose of this calculation, one can use the well known parametrizations of Cugnon [20] for the free space elastic and inelastic nucleon-nucleon cross sections as a function of the available center of mass energy, $\sqrt{s}$, in a nucleon-nucleon collision.

$$\begin{aligned} \sigma_{\rm el}(\sqrt{s}) &= \frac{35}{1 + 100(s - 1.8993)} + 20, \quad (\sqrt{s} > 1.8993) \\ \sigma_{\rm inel}(\sqrt{s}) &= \frac{20(\sqrt{s} - 2.015)^2}{0.015 + (\sqrt{s} - 2.015)^2}, \quad (\sqrt{s} > 2.015). \end{aligned} \tag{34}$$

In this parameterization, $\sqrt{s}$ is measured in GeV and σ in mb.

In Fig. 2(b), we display the results for $\overline{\sigma}_{\rm inel}(E_{\rm beam})$ and $\overline{\sigma}_{\rm total}(E_{\rm beam})$ for three different cases. The solid lines are for free nucleons. In this case, the distribution function f are δ-functions, and we have $\overline{\sigma}(E_{\rm beam}) = \sigma_{NN}$. The threshold energy for pion production is in this case $E^{\rm th}_{\rm beam}$/nucleon = 290 MeV.

The dashed and dotted lines represent the case that the target is a carbon nucleus. $f_A(\mathbf{p})$ is then a Fermi gas distribution function with Fermi momentum of 221 MeV/c determined from the carbon fragmentation experiment. The dashed lines are obtained by using the momentum distribution of ^{11}Li core neutrons for f_B, and the dotted line represents the case that the halo neutron momentum distribution is used. In these cases, the threshold energies for pion production are 70 MeV and 120 MeV, respectively.

One can see from Fig. 2(b) that the distribution averaged value of the total nucleon-nucleon cross section is hardly affected by the momentum distribution of nucleons in target and projectile. However, the averaged inelastic cross section shows a very large effect close to the threshold.

In Table 9.2, one sees the results for the ratio

$$E = \frac{\sigma^{\pi^-}_{\rm inc} - \sigma^{\pi^+}_{\rm inc}}{\sigma^{\pi^-}_{\rm inc} + \sigma^{\pi^+}_{\rm inc}} \tag{35}$$

for the systems ^{A}Li + ^{12}C (A = 7, 8, 9, 11) with $\overline{\sigma}$ = 40 mb and 25 mb. These two values for $\overline{\sigma}$ are chosen to represent the case for nucleus-nucleus interactions around the pion production threshold ($E_{beam} \approx 200$ MeV/nucleon $\rightarrow \overline{\sigma} \approx 25$ mb) and for reactions at higher beam energies ($E_{beam} \approx 800$ MeV/nucleon $\rightarrow \overline{\sigma} \approx 40$ mb). For comparison, we also present the ratio E_0 for the two cross section which results from simple counting arguments of neutrons and protons or, equivalently, from assuming that protons and neutrons have the same density distribution in Eq. 35,

$$E_0 = \frac{N_A N_B - Z_A Z_B}{N_A N_B + Z_A Z_B}. \tag{36}$$

The ratio E is sensitive to the difference between proton and neutron density distribution [12].

	^{7}Li+^{12}C	^{8}Li+^{12}C	^{9}Li+^{12}C	^{11}Li+^{12}C
E(40mb)	0.1153	0.2221	0.2955	0.3951
E(25mb)	0.1143	0.2210	0.2939	0.3927
E_0	0.1429	0.2500	0.3333	0.4545

Table 9.2: Comparison of the computed normalized cross section differences between negative and positive pion production, E, for two different values of $\overline{\sigma}$ and the same quantity obtained from simple counting of nucleons, E_0, for reactions of different Li isotopes with ^{12}C.

0.4 Pion energy spectra

If we want to study pion energy spectra, it is clearly not sufficient any more to use energy averaged production cross sections. In an exploratory study of pion spectra with exotic nuclei, a modified Fermi gas model can be used. It was first used by G. Bertsch in the study of threshold pion production [21].

For the individual nuclei, we assume that the phase space distribution function can be separated into coordinate and momentum parts. For the momentum space distribution of the colliding nuclei we use a simplified form of two homogeneously filled Fermi spheres, the centers of which are separated by the beam momentum

$$f_{AB}(\mathbf{p}) = \theta(p_{f_A} - |\mathbf{p}|)A + \theta(p_{f_B} - |\mathbf{p} - \mathbf{p}_{beam}|)B. \tag{37}$$

Here p_{f_A} and p_{f_B} are the Fermi momenta of the projectile of mass A and target of mass B respectively. We will use the Fermi momenta for carbon and ^{11}Li extracted from the experimental data as we have discussed in the previous Section.

Pion energy spectra in the reaction $A + B$ can then be calculated as a sum of the pion energy distribution in each nucleon-nucleon collision with all possible momenta within the

Fermi spheres

$$\left(\frac{d\sigma_\pi}{dE}\right)_{AB} = C \int \left(\frac{d\sigma_\pi(s)}{dE}\right)_{NN} f_A(\mathbf{p}_A) f_B(\mathbf{p}_B) d^3p_A d^3p_B, \tag{38}$$

where C is a constant coming from the integration over the impact parameter, which is irrelevant for the following discussions. s is the square of the center of mass energy of the two colliding nucleons.

To calculate the pion energy distribution $(d\sigma_\pi/dE)_{NN}$ in each nucleon-nucleon collision, we assume that pion production is proceeding via the Δ resonance. The mass distribution of the Δ resonance is taken from Y. Kitazoe et. al. [19] and is given by

$$P(M_\Delta) = \frac{0.25\,\Gamma^2(q)}{(M_\Delta - M_0)^2 + 0.25\,\Gamma^2(q)}, \tag{39}$$

where $M_0 = 1232$ MeV, and the width Γ(q) of the resonance is parametrized as

$$\Gamma(q) = \frac{0.47 q^3}{[1 + 0.6(q/m_\pi)^2]\, m_\pi^2}. \tag{40}$$

q is the pion-momentum.

The Δ is assumed to be produced isotropically in the nucleon-nucleon center of mass frame, and one can also assume that the decay of the resonance has an isotropic angular distribution in the Δ rest frame. The decay of the resonance can then be calculated using a Monte Carlo integration technique. This leads to a pion energy spectrum in the Δ rest frame which is finally Lorentz transformed into the laboratory frame.

The integration in Eq. 38 for calculating the pion spectra in the reaction $A + B$ can be performed with a Monte Carlo integration method. One generates pairs of colliding nucleons from the projectile and the target, and isospin quantum numbers are assigned to these nucleons according to the N/Z ratios of the projectile and the target. Then, one can use available experimental data [18, 22] for pion production cross sections in nucleon-nucleon collisions in all possible isospin channels.

One such calculation is performed for the reaction ^{11}Li+^{12}C at various beam energies. To show the sensitivity of the pion energy spectra on the nucleon momentum distribution of the radioactive nuclei, Fig. 3(a) shows the π^- spectra calculated by using the core Fermi momentum and halo Fermi momentum for the ^{11}Li projectile, respectively. The solid histograms are calculated with $p_{f_A} = p_f$(halo) = 38 MeV/c and the dotted histograms are calculated with $p_{f_A} = p_f$(core) = 158 MeV/c. These two calculations simulate the situations that nucleons coming from ^{12}C collide with the halo and core nucleons of the ^{11}Li, respectively [14].

A strong sensitivity of the pion spectra to the nucleon momentum distribution can be seen, in particular for beam energies smaller than about 300 MeV/nucleon. Moreover, the

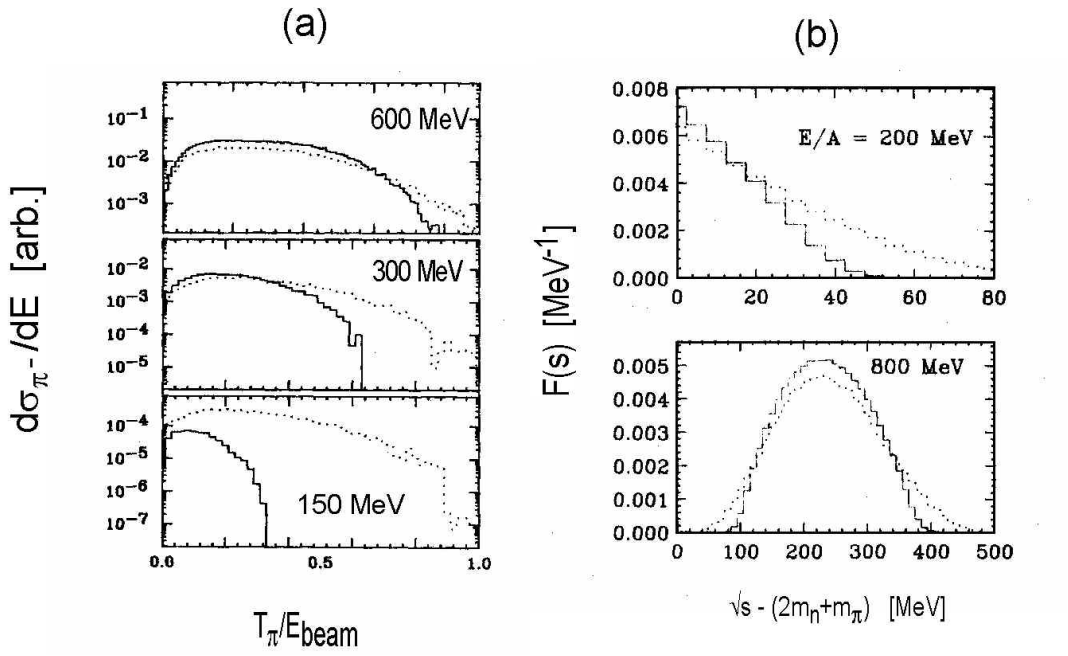

Figure 3: (a) π^- kinetic energy spectra in the reaction ^{11}Li+^{12}C at beam energies of 600, 300 and 150 MeV/nucleon. The solid lines are calculated with $p_{f_A} = p_f$(halo) and the dotted lines are calculated with $p_{f_A} = p_f$(core). (b) Distribution of the center of mass energy above pion production threshold for pairs of colliding nucleons in the reaction ^{11}Li+^{12}C. The solid and dotted lines are calculated under the same conditions as in (a).

different slopes of the two curves indicate that the different momentum distributions of core and halo neutrons can be seen experimentally.

Of course, one needs to know how to disentangle the pions produced by the core and by the halo neutrons. One can do this in two ways: First, one can separate central and peripheral collisions via some impact parameter trigger. Since the halo neutrons should contribute stronger to pion production in peripheral collisions, their effect can be isolated. A second and more tractable way to isolate the effect of the halo neutrons is a subtraction method. Here one can utilize the fact that a ^{9}Li nucleus contains the same core neutrons as ^{11}Li. Thus, if one subtracts the pion spectrum produced in a ^{9}Li induced reaction from that of a ^{11}Li induced and otherwise identical reaction, the pion spectrum due to the halo neutrons can be obtained.

Presently available radioactive beam facilities can produce high quality ^{11}Li and ^{9}Li beams. Using these, the different neutron momentum distributions of core and halo neutrons in ^{11}Li shows up as contributions to the pion energy spectra with different slopes in ^{11}Li and

^{9}Li induced reactions. One estimates [14] that a beam of 10^5 ^{11}Li per second at a beam energy of 300 MeV/nucleon would produce about 10^4 pions per second. With this production rate, a high quality experiment using a pion spectrometer can be performed.

As can be seen from Fig. 3(a), the difference in the slope of the pion spectra is not so obvious at beam energies above 600 MeV/nucleon. This can be understood by looking at the distribution of the center of mass energy, $\sqrt{s}$, of the two colliding nucleons in the reaction $A + B$

$$F(s) = \int f_A(\mathbf{p}_A) f_B(\mathbf{p}_B - \mathbf{p}_{beam}) \delta(s - 2m_n^2 - 2E_A E_B + 2\mathbf{p}_A \cdot \mathbf{p}_B) d^3p_A d^3p_B. \qquad (41)$$

Here we take on-shell nucleons so that $E_i = (p_i^2 + m_n^2)^{1/2}$ for $i = A, B$.

In Fig. 3(b) we present the distribution of $\sqrt{s} - (2m_n + m_\pi)$, which is the total available center of mass energy above pion production threshold in nucleon-nucleon collisions. The calculation was done [14] for the reaction ^{11}Li + ^{12}C at beam energies of 200 MeV/nucleon and 800 MeV/nucleon. Again, the solid histograms are the results using $p_{f_A} = p_f$(halo) and the dotted ones using $p_{f_A} = p_f$(core). The effect of different internal momentum distributions is obvious at lower energies, but as the beam energy gets much larger than the pion production threshold energy, the effect becomes less obvious.

One can thus see that pion production with radioactive nuclei provides an alternative way for further determination of the properties of exotic nuclei.

Bibliography

[1] G.F. Bertsch, B.A. Brown and H. Sagawa, Phys. Rev. C **39** (1989) 1154.

[2] P.G. Hansen and B. Jonson, Europhys. Lett. **4** (1987) 409.

[3] T. Kobayashi et al., Phys. Rev. Lett. **60** (1988) 2599.

[4] A.S. Goldhaber, Phys. Lett. **53B** (1974) 306.

[5] C.A. Bertulani and M.S. Hussein, Phys. Rev. Lett. **64** (1990) 1099.

[6] R. Anne, S.E. Arnell, R. Bimbot, H. Emling, D. Guillemaud-Mueller, P.G. Hansen, L. Johannsen, B. Jonson, M. Lewitowicz, S. Mattsson, A.C. Mueller, R. Neugart, G. Nyman, F. Pougheon, A. Richter, K. Riisager, M.G. Saint-Laurent, G. Schrieder, O. Sorlin and K. Wilhelmsen, Phys. Lett. **B250** (1990) 19.

[7] D. Guillemaud-Müller and A.C. Müller, "NSCL Seminars on Experimantal Techniques: 1. Exotic Nuclei", Michigan State University Report MSUCL-742.

[8] B.-A. Li and W. Bauer, Phys. Lett. **B254** (1991) 335.

[9] W. Bauer, Phys. Rev. **C40** (1989) 715.

[10] W. Cassing, et al., Phys. Rep. **188** (1990) 363.

[11] A. Bonasera, F. Gulminelli and J. Molitoris, Phys. Rep. **243** (1994) 1.

[12] R.J. Lombard and J.P. Maillet, Europhys. Lett. **6** (1988) 323.

[13] A. Tellez, R.J. Lombard and J.P. Maillet, J. Phys. **G13** (1987) 311..

[14] B.-A. Li, W. Bauer and M.S. Hussein, Nucl. Phys. **A533** (1991) 749.

[15] C.Gale, G.Bertsch and S. Das Gupta, Phys. Rev. **C35** (1987)1666.

[16] C. Gregoire et al, Nucl.Phys. **A465** (1987)317.

[17] P.J. Karol, Phys. Rev. **C11** (1975) 1203.

[18] B.J. VerWest and R.A. Arndt, Phys. Rev. **C25** (1980) 1979.

[19] Y. Kitazoe et. al., Phys. Lett. **166B** (1986) 35.

[20] J. Cugnon, T. Mizutani and J. Vandermeulen, Nucl. Phys. **A352** (1981) 505.

[21] G.F. Bertsch, Phys. Rev. **C15** (1977) 713.

[22] W.O. Lock and D.F. Measday, Intermediate Energy Nuclear Physics (Methuen, London, 1970).